Metal-Porphyrin Complexes: A DFT Study of Hydrogen Adsorption and Storage

Ahmet Kose, Numan Yuksel, M. Ferdi Fellah [1]

Department of Chemical Engineering, Bursa Technical University, Mimar Sinan Campus, 16310, Bursa, Turkey.

Abstract: It has been performed hydrogen adsorption on four metallo-porphyrin complexes by Density Functional Theory (DFT) calculations at room temperature. The WB97XD hybrid formalism method was used for hydrogen adsorption on metallo-porphyrin complexes formed with alkaline metal and alkaline earth metal (Na, K, Mg and Ca) atoms. It was determined that the adsorption energies for all complexes were negative, so that each of them could be a potential adsorbent for hydrogen storage. The adsorption enthalpy (ΔH) was calculated as -21.9 kJ/mol for the Na-Porphyrin (Na-P) complex structure. Moreover, the gravimetric hydrogen storage capacity for the Na-P complex was calculated to be ≈5.5 wt%. Thus, the DOE's target for 2025 has been achieved. In addition, van der Waals weak interactions were found to be effective in hydrogen adsorption and storage studies. Based on the electronic properties the metallo-porphyrin complexes could not be used as electronic sensors against the hydrogen molecule.

1. Introduction

As is well known, hydrogen is seen as a cleaner alternative to polluting fossil fuels [1]. Scientific studies on storage, which is the most significant of the production, transportation, storage, and application processes, are still ongoing. Much research have been devoted to technologies that have the potential to meet set hydrogen storage targets, led by the US Department of Energy (US DOE). According to the US DOE, a system with hydrogen gravimetric (5.5% by weight) and volumetric capacity (0.040 kg H_2/L) for a target driving range of 300 miles by 2025 should be developed [2].

Metal organic frameworks (MOFs), covalent organic frameworks (COFs) and zeolites, among other ultrafine nanoporous materials, have been extensively studied in recent decades [3]. MOFs are highly porous crystal structures with a large surface area that have the potential to capture huge amounts of gas molecules in their cavities. With the addition of heat or pressure, the hydrogen adsorbed by the weekly van der Waals force on the pores of the MOFs can be rapidly desorbed [4]. Porphyrin, a member of the macrocyclic class, is a MOF that can complex with metal atoms and is effective in gas studies [5,6]. MOFs are popular materials that have been used extensively in hydrogen storage studies in recent years [7-9]. In our recent study, the IRMOF-16 structure was decorated with Mg atom and the hydrogen storage capacity was determined as 5.8 wt% [10]. Additionally, metal porphyrins can be synthesized as microporous solid frameworks with selective sorption of small molecules (like H_2 molecule) and heterogeneous catalysis based on size or shape [11]. Porphyrins offer powerful electron-donor characteristics due to the four nitrogen atoms in the tetrapyrrolic core [12]. Owing to its large aggregation capabilities, charge transfer abilities, wide variety of derivatizability and other properties, metallo-porphyrin has recently caught the interest of researchers in the area of adsorption, sensors, catalysis and many others [13-15]. Metal porphyrins are also studied for the hydrogen evolution reaction and hydrogen production [16-18]. These macrocyclic organic compounds have a wide range of uses, including gas reduction and oxidation, gas capture and storage, and more [19].

---

[1] Corresponding Author

e-mail: mferdi.fellah@btu.edu.tr

In the literature, there are many studies in which hydrogen adsorption is increased by decorating metal atoms on nanomaterials [20-25]. The most commonly used metal atoms are alkaline and alkaline earth metals such as Li, Na, K, Be, Mg and Ca. The computational chemistry is very important for the development of new hydrogen storage materials [26]. In the study, in which Monte Carlo method and DFT method were used together, the hydrogen storage capacities of Mg-porphyrin, Ca-porphyrin and Sc-porphyrin-based nanosheets at 298 K and 100 bar were determined as 1.25 wt%, 3.99 wt% and 6.71 wt%, respectively [27]. In another research, hydrogen storage works for Porphyrin-like porous Fullerene structure ($C_{24}N_{24}$) decorated with Sc, Ti and V transition metals were carried out by DFT method. The results show that the highest gravimetric capacity (≈5.1 wt%) was achieved with the Sc decorated structure ($C_{24}N_{24}Sc_6$) [28]. In a hydrogen adsorption study, using DFT method with a pyridine bridged porphyrin-covalent organic framework structure; the highest gravimetric capacity was calculated as ≈5.1 wt% at 298 K and 100 bar [29].

In this study, hydrogen adsorption was carried out theoretically on metallo-porphyrin complexes, which there are not many studies in the literature, and the gravimetric storage capacity was determined for the structure with the best adsorption values. The WB97XD hybrid method was utilized in the calculations carried out with the DFT method. Here, alkaline (Na, K) and alkaline earth (Mg, Ca) metal atoms were used in metallo-porphyrin complexes.

2. Computational Method

DFT calculations [30] were performed using Gaussian09 software [31] to obtain optimized geometries and electrical properties. The WB97XD (including dispersion) hybrid formalism method was used to account for the effects of change and correlation [32]. The WB97XD density functional was previously reported to be the most compatible method with experimental H_2 adsorption, and it was determined that there was a difference of 1.1 kcal/mol from the experimental data [33]. The 6-31G(d,p) basis set was used in computations for all atoms. The complex formations were realized by replacing one metal atom with two hydrogen molecules at the center of the porphyrin structure.

Four metallo-porphyrin complexes that could interact with the hydrogen molecule have been used in this research. These four complexes are Na-Porphyrin (Na-P), K-Porphyrin (K-P), Ca-Porphyrin (Ca-P) and Mg-Porphyrin (Mg-P). DFT calculations were used to optimize the geometries (to obtain the Equilibrium Geometry (EG)) and obtain energy values for adsorption. In this analysis, zero-point energy (ZPE) corrections are included in the energy values. All atoms have been kept relaxed during all theoretical calculations. In present study, the basis-set superposition error (BSSE) correction using the counterpoise method has not been taken into account because it generally has small effects (approximately 1 kcal/mol) on the calculations [34,35]. The following equation was used to calculate the adsorption energy and enthalpy values of the metallo-porphyrin (M-P) complexes against the H_2 molecule.

$$\Delta(E/H) = (E/H)_{System} - [(E/H)_{M-P} + (E/H)_{H2}] \qquad (1)$$

where $(E/H)_{System}$ is the thermal energy/enthalpy of H_2 on the complex, $(E/H)_{H2}$ is the hydrogen molecule's thermal energy/enthalpy and $(E/H)_{M-P}$ is the initial thermal energy/enthalpy of M-P complex. Information on the calculation of E and H values have been given in Supplementary Material (SM). Details of computational method utilized in this study have been stated in SM.

3. Results and discussion

First, Na-P, K-P, Mg-P and Ca-P complexes were optimized to obtain optimized EGs by DFT method. EGs of M-P complexes were determined by taking the total charge as zero and the SM (Spin Multiplicity) as singlet and doublet. In this respect, it was determined as doublet for Na-P and K-P complexes and singlet for Mg-P and Ca-P complexes. The EG of hydrogen molecule was obtained by taking the total charge as zero and SM as a singlet. The optimized geometries of the M-P complexes are shown in Fig. 1. To confirm the accuracy of WB97XD hybrid method and the 6-31G(d,p) basis set, the Mg-N bond length of the Mg-P complex in this study was compared with the Mg-N bond length of the Mg-Porphyrin-based complexes from the previously reported experimental studies. Experimentally, it has been reported that Mg-N bond lengths in Mg-Porphyrin-based structures range from 2.062 Å to 2.072 Å

[36,37]. In present study, the Mg-N bond length in the Mg-P complex was calculated as 2.057 Å. These results show that the structural parameters of the WB97XD hybrid method and the 6-31G(d,p) basis set are very close to the experimental results.

The bond lengths between the metal atom and nitrogen atoms in other optimized M-P complexes are as follows; Na-N, K-N and Ca-N bond lengths were calculated as 2.133 Å, 2.647 Å and 2.329 Å, respectively.

Na-P complex

K-P complex

Mg-P complex
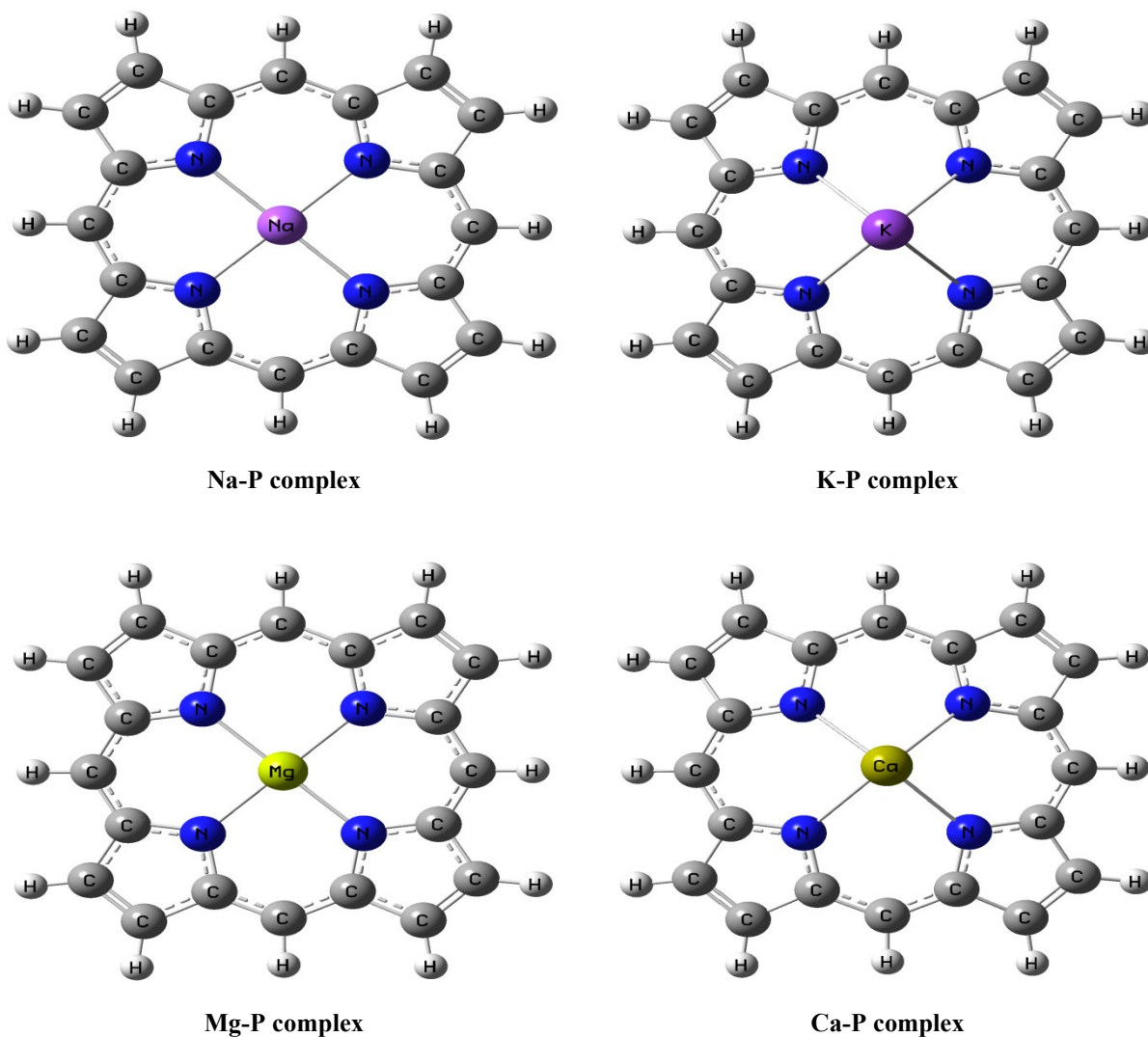
Ca-P complex

Fig. 1 The optimized geometries of the M-P complexes.

After obtaining the EGs of both hydrogen molecule and M-P complexes separately, optimization calculations were made for the adsorption of hydrogen molecule of the complexes. The optimized geometries of the hydrogen-adsorbed M-P complexes have been represented in Fig. 2. The adsorption energy values for H_2 molecule adsorption on Na-P, K-P, Mg-P and Ca-P complexes were listed in Table 1.

When the adsorption energy (ΔE) and adsorption enthalpy (ΔH) values were examined, negative values were obtained for all M-P complexes. This result indicates that the hydrogen molecule adsorption on the M-P complexes are an exothermic process at room temperature. Moreover, the adsorption enthalpy values on these complexes are lower than the liquefaction enthalpy (0.9 kJ/mol) of the hydrogen molecule [38]. Thus, all four M-P complexes have some potential as adsorbent structure at room temperature. The best adsorption values are seen for the Na-P complex, and the ΔE and ΔH values on this structure have

been computed to be -19.5 kJ/mol and -21.9 kJ/mol respectively.

In order to investigate the electronic properties of M-P complexes against hydrogen molecule, HOMO (Highest Occupied Molecular Orbital) and LUMO (Lowest Unoccupied Molecular Orbital) energies were calculated and the change in HOMO-LUMO gap energy (E_g) values was examined. The HOMO, LUMO and E_g values of the M-P complexes before and after adsorption are listed in Table 2. In addition, for M-P complexes (Na-P and K-P) with doublet SM, both α and β molecular orbitals (spin up and spin down, respectively) were calculated.

H₂/Na-P complex   H₂/K-P complex

H₂/Mg-P complex   H₂/Ca-P complex
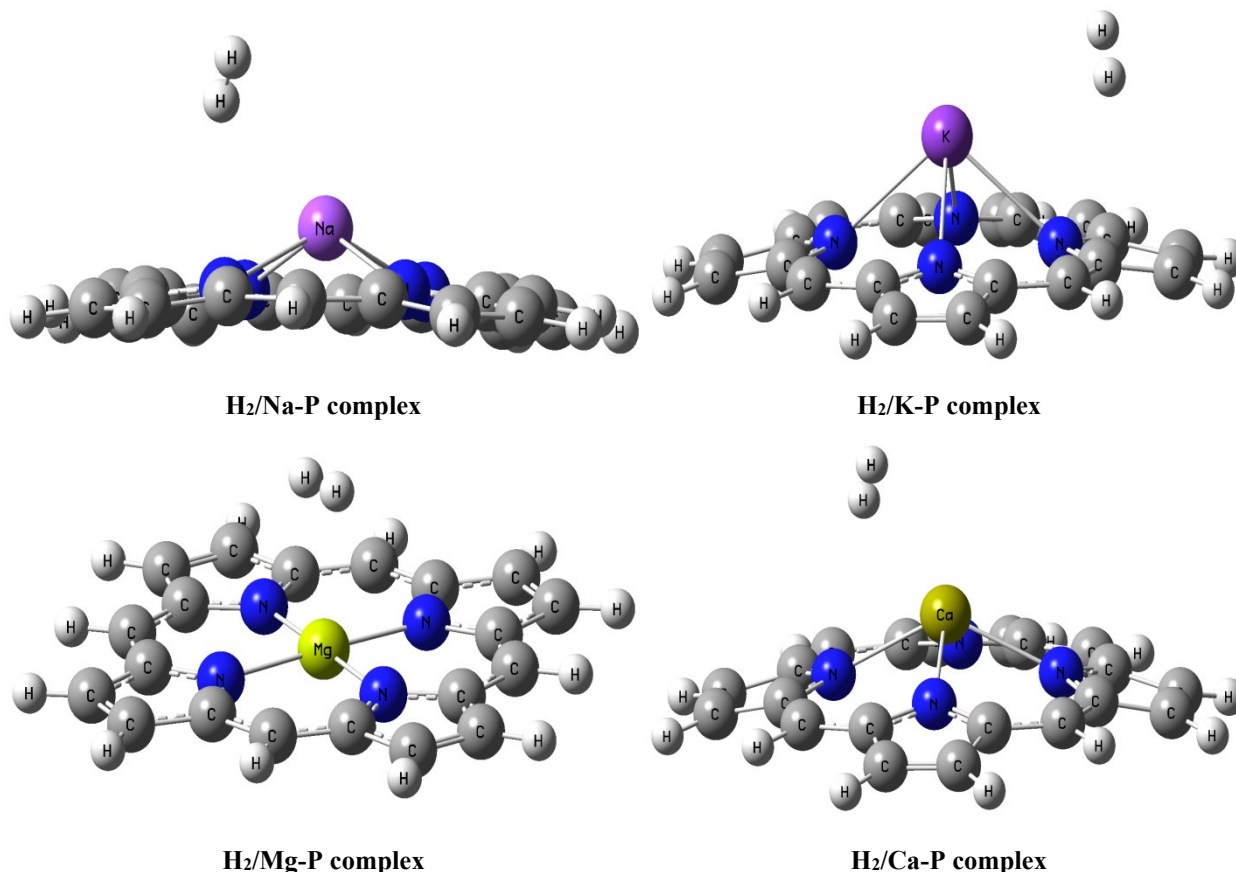
Fig. 2 The optimized geometries of the H₂ adsorbed M-P complexes.

Table 1. Adsorption energy and enthalpy values for H₂ adsorption on M-P complexes (values are in units of kJ/mol).

Properties	Na-P Complex	K-P Complex	Mg-P Complex	Ca-P Complex
ΔE	-19.5	-1.9	-4.4	-6.5
ΔH	-21.9	-4.4	-6.9	-9.0

The E_g has been repeatedly recognized and supported to be a good indicator for evaluating the sensitivity of nanosensors [39]. There is also a relation between E_g and electrical conductivity (σ), which has also been mentioned [40,41]:

$$\sigma = AT^{3/2} \exp\left[-E_g/(2\kappa T)\right] \qquad (2)$$

where κ is the Boltzmann's constant, A (electrons/m³K^{3/2}) is a constant and T is temperature. Many papers have demonstrated that the findings of utilizing this formula are supported by experimental studies [42,43]. The Eq. (2) shows when E_g decreases, the population of conduction electrons increases exponentially. As a result, the chemical's presence in the environment improves electrical conductivity. According to the results in Table 2, the E_gs of Na-P and K-P complexes increase after adsorption, while there are some negligible decrease in Mg-P and Ca-P complexes. Therefore, it turns out that the M-P complexes in this study cannot be used as electronic sensors since

there is no significant reduction in ΔE_gs. In addition, atomic charge distributions before and after adsorption were obtained through Mulliken population analysis and are listed in Table 2. Accordingly, the charges of the metal atoms in all complexes decreased, and the total charge of the adsorbed hydrogen molecule increased. These results show that metal atoms gain electrons, while hydrogen molecule donates electrons and there is charge transfer between them.

Chemical hardness (η), chemical potential (μ) and electronegativity (χ) were calculated (details on calculations are in SM) for all complexes and listed in Table 3. Looking at the results, no significant change was observed in general. This result shows that the complexes maintain their stability after adsorption. However, if we need to compare with each other, it has been seen that Na-P and K-P complexes can be harder after adsorption, whereas Mg-P complex can be softer.

Additionally, it can be said that there is no change in the Ca-P complex. Fig. 3 presents HOMO and LUMO representations of the Na-P complex and the hydrogen molecule adsorbed Na-P complex. For the other M-P complexes, the HOMO and LUMO representations before and after adsorption are given in Fig. S1, Fig. S2 and Fig. S3 in SM. According to the HOMO-LUMO analysis, there is no change in both HOMOs and LUMOs before and after adsorption for all complexes. This situation is attributed to low charge transfer.

Table 2. Electronic properties of M-P complexes and H_2/M-P systems, including energies of HOMO and LUMO, E_g and ΔE_g (values are in units of kJ/mol). The charges of both metal atoms and hydrogen molecule are shown before and after adsorption (in units of e).

Structure		E_{HOMO}	E_{LUMO}	E_g	ΔE_g	Metal atom Charge	H_2 Charge
Na-P Complex	α MOs	-612.8	-98.3	514.5	-	+0.659	-
	β MOs	-663.7	-213.4	450.3	-		
H_2/Na-P Complex	α MOs	-602.9	-85.5	517.4	2.9	+0.615	+0.013
	β MOs	-666.2	-206.8	459.3	9.0		
K-P Complex	α MOs	-584.4	-65.2	519.2	-	+0.707	-
	β MOs	-647.6	-185.1	462.6	-		
H_2/K-P Complex	α MOs	-586.7	-67.4	519.3	0.1	+0.697	+0.008
	β MOs	-649.6	-186.5	463.1	0.5		
Mg-P Complex	$\alpha+\beta$ MOs	-639.9	-78.7	560.2	-	+0.911	-
H_2/Mg-P Complex	$\alpha+\beta$ MOs	-637.3	-77.5	559.8	-0.4	+0.900	+0.027
Ca-P Complex	$\alpha+\beta$ MOs	-610.5	-55.5	555.1	-	+1.301	-
H_2/Ca-P Complex	$\alpha+\beta$ MOs	-610.9	-56.2	554.7	-0.4	+1.271	+0.019

Table 3. Chemical hardness, chemical potential and electronegativity values for the optimized M-P complexes and H_2/M-P systems (values are in units of kJ/mol).

Structure		Chemical hardness (η)	Chemical potential (μ)	Electronegativity (χ)
Na-P Complex	α MOs	257.2	-355.6	355.6
	β MOs	225.1	-438.6	438.6
H_2/Na-P Complex	α MOs	258.7	-344.2	344.2
	β MOs	229.7	-436.5	436.5
K-P Complex	α MOs	259.6	-324.8	324.8
	β MOs	231.3	-416.3	416.3
H_2/K-P Complex	α MOs	259.6	-327.1	327.1
	β MOs	231.5	-418.1	418.1
Mg-P Complex	$\alpha+\beta$ MOs	280.1	-358.8	358.8
H_2/Mg-P Complex	$\alpha+\beta$ MOs	279.9	-357.4	357.4
Ca-P Complex	$\alpha+\beta$ MOs	277.5	-333.0	333.0
H_2/Ca-P Complex	$\alpha+\beta$ MOs	277.4	-333.5	333.5

The density of states (DOS) plots of M-P complexes before and after adsorption are presented in Fig. 4. Looking at Fig. 4, there was no significant change in DOS plots. In particular, it is shown that there is no reduction in band gap after hydrogen adsorption of M-P complexes. This result confirms the ΔE_g values in Table 2 and indicates that these complexes cannot be electronic sensors for hydrogen detection. Fig. 5 shows the electrostatic potential (ESP) distribution of H_2

Ahmet Kose, Numan Yuksel, M. Ferdi Fellah

adsorbed M-P complexes. On the ESP maps, the positive and negative areas of the Van der Waals surface corresponded to blue and red colors, respectively [44,45]. The ESP distributions are mapped to a constant electron density region. ESP decreases with different colors, red < yellow < green < blue. According to the ESP analysis, it is understood that blue-green colors dominate, therefore there is a positive electrostatic potential in the interaction between M-P complexes and the hydrogen molecule. Thus, the absence of red colors, that is, the absence of negative electrostatic potential, visually reveals that there is very low electron exchange.
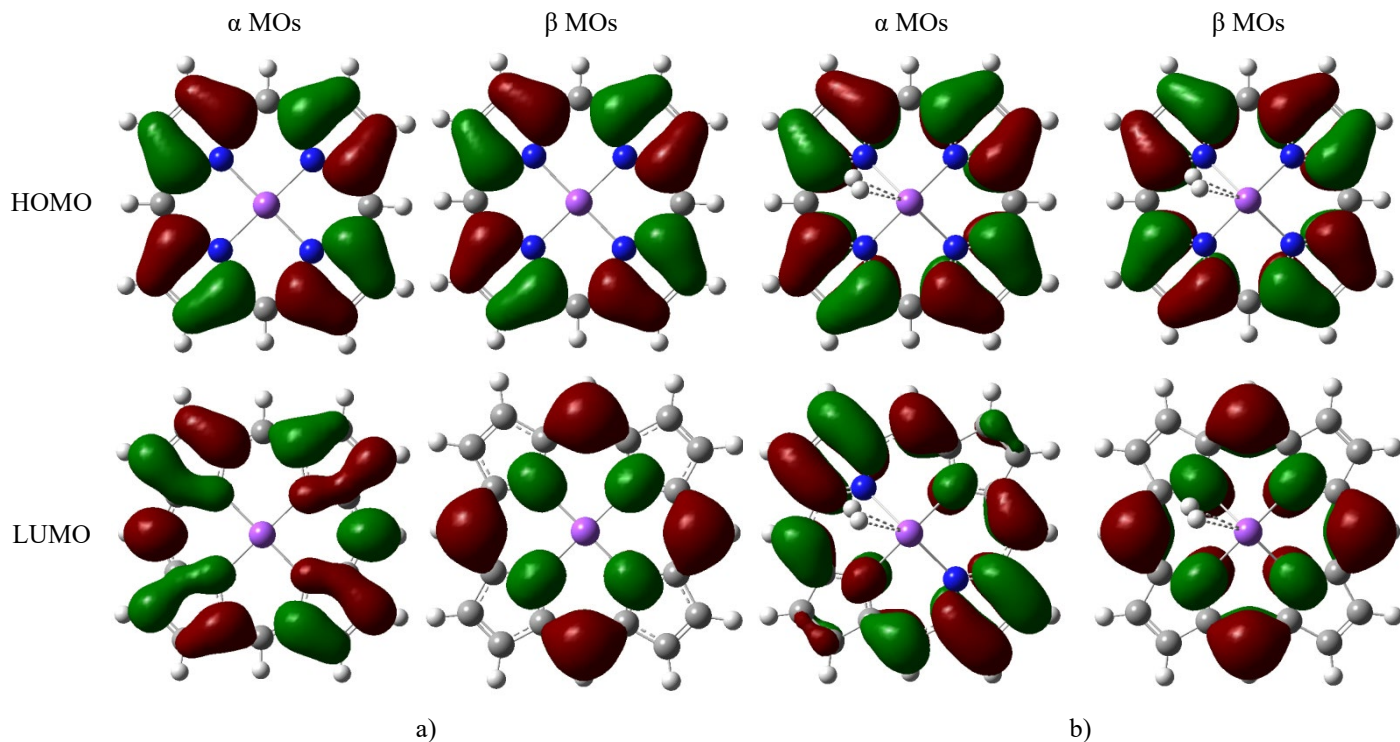
Fig. 3 The representations HOMO / LUMO distributions of α and β MOs for the Na-P complex of a) before and b) after H_2 adsorption.
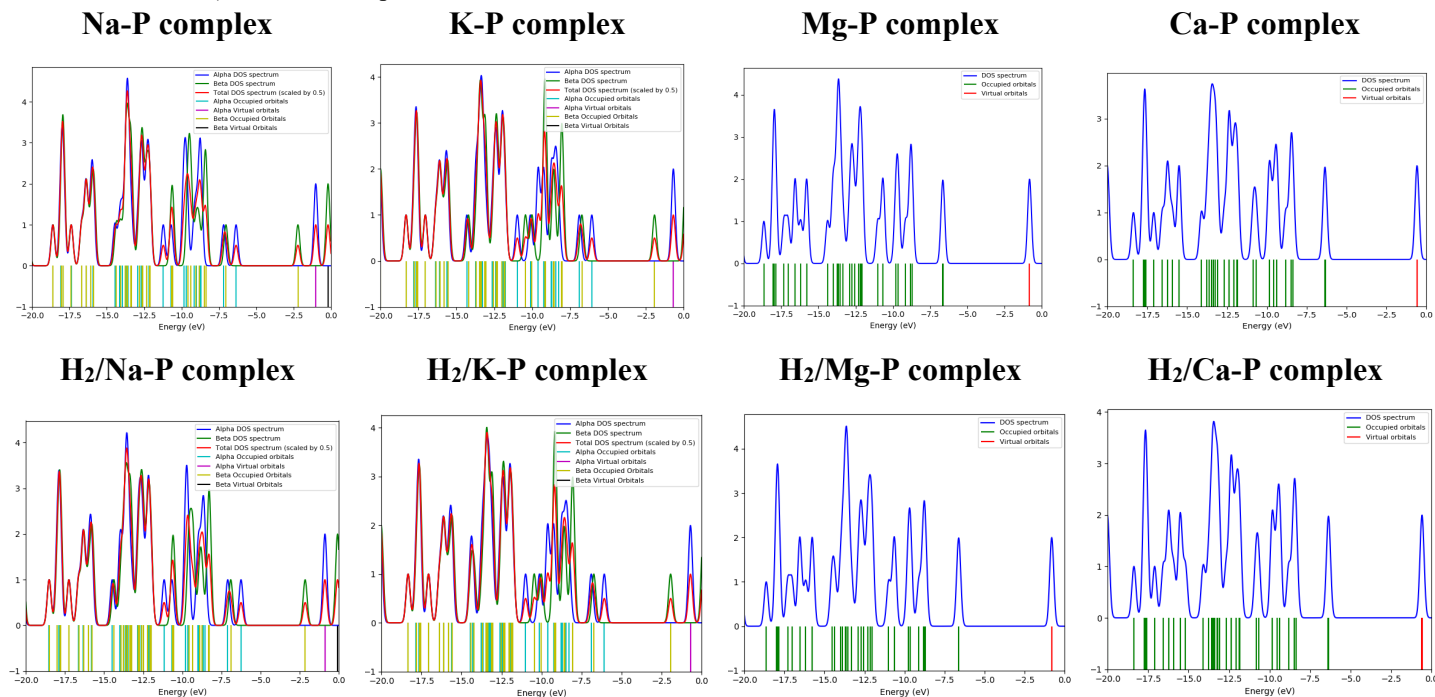
Fig. 4 Density of states (DOS) plots for the optimized structures.

H₂/Na-P Complex   **H₂/K-P complex**

H₂/Mg-P complex   **H₂/Ca-P complex**
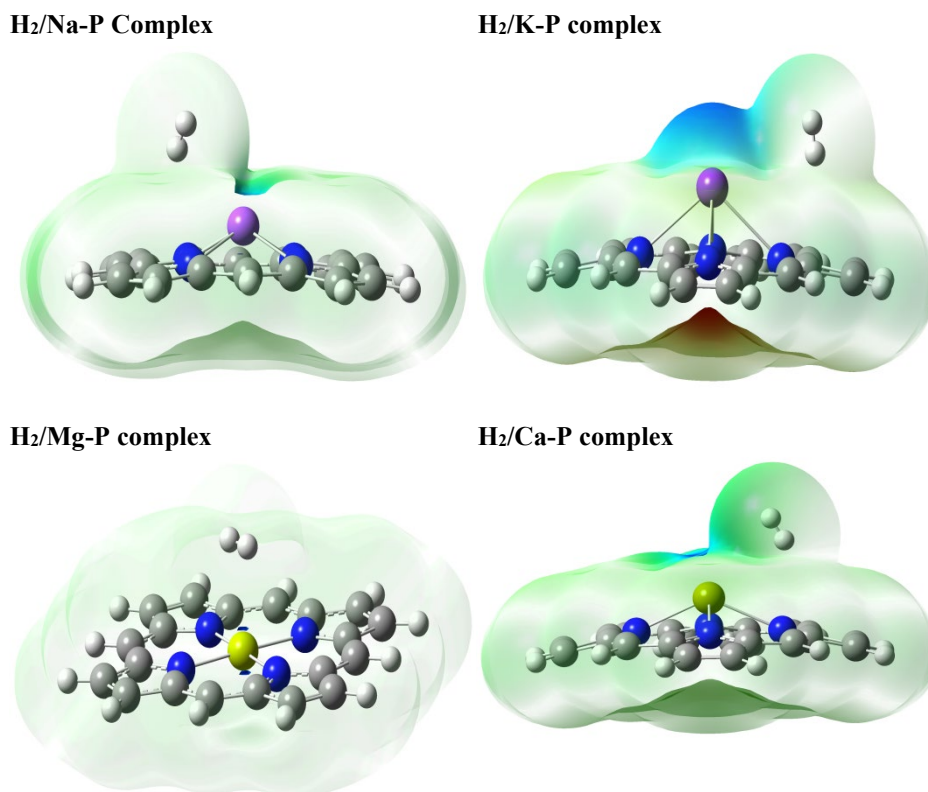
Fig. 5 Electrostatic potential (ESP) distributions for the optimized structures of the M-P complexes with adsorbed hydrogen molecule.
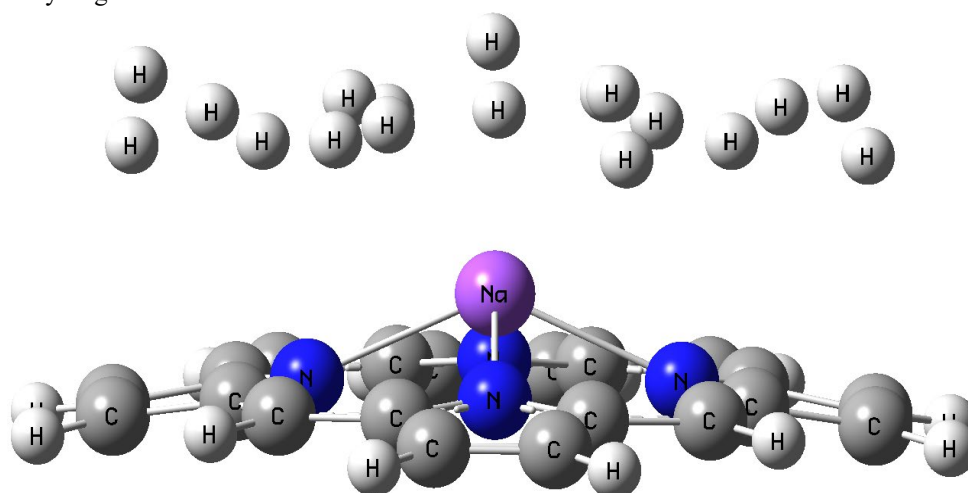
Fig. 6 Optimized geometry for the structure of the Na-P complex with nine adsorbed H₂ molecules.

A storage study has been conducted for the Na-P complex that gives the best adsorption result for hydrogen adsorption. In other words, by adding more than one hydrogen molecule, it was found out how many hydrogen molecules adsorbed on the Na-P complex. This process continued until the last hydrogen molecule that it would not adsorb. With each addition of hydrogen molecule, the adsorption enthalpy change approaches positive values. Eventually, its complex structure pushed the tenth hydrogen molecule. Nine H₂ molecules have been adsorbed on the Na-P complex, and the optimized structure were shown in Fig. 6. The gravimetric hydrogen storage capacity of the complex was calculated as ≈5.5 wt% by using Eq. (3). Thus, it has been reached to the gravimetric hydrogen storage capacity determined by DOE for 2025.

$$H_2 \, wt\% = [M_{H2}/(M_{H2}+M_{Na\text{-}P})]x100 \quad (3)$$

In this equation, M_{H2} is the mass of the adsorbed hydrogen molecules on Na-porphyrin complex and M_{Na-P} is the mass of Na-porphyrin complex. If we compare the gravimetric hydrogen storage studies at 100 bar of porphyrin-based materials given in the introduction section, we can say that the calculated result for the Na-P complex at atmospheric pressure is better. Furthermore, due to the derivatizability of porphyrin compounds with different functional groups, one could mention that hydrogen storage capacity can be increased by forming complexes with more metal atoms.

Finally, reduced density gradient (RDG) analysis was performed for the Na-P complex, where the maximum hydrogen uptake was reached. The RDG analysis has been proposed by Johnson's et al. group [46], which allows obtaining the type of interactions occur between two species (Na-P and H_2). This analysis has been used to examine the many noncovalent interactions remaining in the molecules, the reduced gradient of the density as a function of the electron density multiplied by the sign of the second eigenvalue of the Hessian matrix. Fig. 7 shows the RDG scatter plot and isosurface for nine H_2 adsorption on Na-P complex. Strong attractive, weak and repulsive interactions have been represented in blue, green and red colors, respectively. Based on the analysis of RDG, for the Na-P complex, the Van der Waals (VdW) interactions are indicated by values near zero as marked by green. The scatter plot of RDG and the isosurface map tell us that the interaction between H_2 molecules and Na-P complex has been typically administrated by weak VdW type interactions.

a)

b)
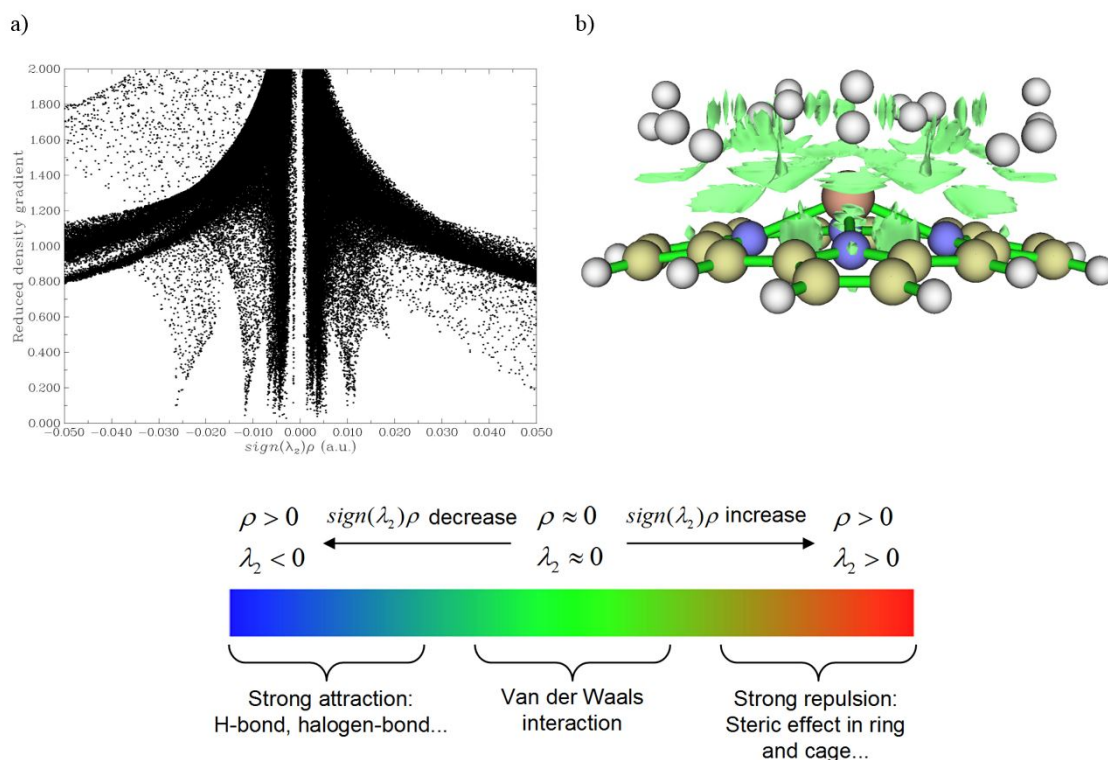
Fig. 7 a) RDG scatter graph and b) RDG isosurface map of nine H_2 adsorption on Na-P complex.

4. Conclusions

In this study, we performed hydrogen adsorption on M-P complexes with DFT calculations. According to the results of the adsorption studies, it was determined that the enthalpy change values for all complexes were negative and lower than the liquefaction enthalpy of the hydrogen molecule. This means that the M-P complexes in this study can be used as a potential adsorbent material in order to store hydrogen at room temperature. Additionally, for the Na-P complex that has the lowest adsorption energy and enthalpy changes hydrogen storage studies were carried out. As a result, the gravimetric storage capacity for the Na-P complex was calculated to be ≈ 5.5 wt%, achieving the DOE's 2025 target. In addition, electronic properties were examined for all complexes before and after adsorption, and it was revealed that these complexes could not be used as hydrogen sensors.

References

[1] E. Baydir, Ö. Aras, Methanol steam reforming in a microchannel reactor coated with spray pyrolysis method for durable Cu/ZnO nanocatalyst, Journal of Analytical Applied Pyrolysis 158 (2021) 105278.

[2] E. Boateng, A., Chen, Recent advances in nanomaterial-based solid-state hydrogen storage, Materials Today Advances 6 (2020) 100022.

[3] Y. Pang, W. Li, J. Zhang, Gas adsorption in Mg-porphyrin-based porous organic frameworks: A computational simulation by first-principles derived force field, Journal Computational Chemistry 38 (2017) 2100-7.

[4] S.P. Shet, S.S. Priya, K. Sudhakar, M. Tahir, A review on current trends in potential use of metal-organic framework for hydrogen storage, International Journal of Hydrogen Energy 46 (2021) 11782-803.

[5] J. Xu, X. Liu, Z. Zhou, M. Xu, Photocatalytic CO2 reduction catalyzed by metalloporphyrin: Understanding of cobalt and nickel sites in activity and adsorption, Applied Surface Science 513 (2020) 145801.

[6] A. Saeidipoor, S. Arshadi, M.R. Benam, The Titano-Porphyrin doped pillared graphene as a novel "turn-off" fluorescent sensor for CO gas: Theoretical study, Physica E: Low-dimensional Systems and Nanostructures 127 (2021) 114554.

[7] H. Gao, R. Shi, Y. Shao, Y. Liu, Y. Zhu, J. Zhang, L. Li, Catalysis derived from flower-like Ni MOF towards the hydrogen storage performance of magnesium hydride, International Journal of Hydrogen Energy 47 (2022) 9346-56.

[8] N. Prasetyo, F.I. Pambudi, Toward hydrogen storage material in fluorinated zirconium metal-organic framework (MOF-801): A periodic density functional theory (DFT) study of fluorination and adsorption, International Journal of Hydrogen Energy 46 (2021) 4222-28.

[9] M.E. Kassaoui, M. Lakhal, A. Benyoussef, A.E. Kenz, M. Loulidi, Enhancement of hydrogen storage properties of metal-organic framework-5 by substitution (Zn, Cd and Mg) and decoration (Li, Be and Na), International Journal of Hydrogen Energy 46 (2021) 26426-36.

[10] N. Yuksel, A. Kose, M.F. Fellah, A DFT investigation of hydrogen adsorption and storage properties of Mg decorated IRMOF-16 structure, Colloids and Surfaces A: Physicochemical and Engineering Aspects 641 (2022) 128510.

[11] P. Maitarad, S. Namuangruk, D. Zhang, L. Shi, H. Li, L. Huang et al., Metal-porphyrin: a potential catalyst for direct decomposition of N(2)O by theoretical reaction mechanism investigation, Environmental Science Technology 48 (2014) 7101-10.

[12] J. Yu, S. Zhu, P. Chen, G-T. Zhu, X. Jiang, S. Di, Adsorption behavior and mechanism of Pb(II) on a novel and effective porphyrin-based magnetic nanocomposite, Applied Surface Science 484 (2019) 124-34.

[13] A.E. Kuznetsov, Hexabenzocoronene functionalized with porphyrin and P-core-modified porphyrin: A comparative computational study, Computational Theoretical Chemistry 1188 (2020) 112973.

[14] X. Du, H. Zhang, Y. Lu, A-H. Wang, P. Shi, Z-S. Li, Fluorination reaction on an inactive sp3 C-H bond mediated by manganese porphyrin catalysts: A theoretical study, Computational Theoretical Chemistry 1115 (2017) 330-334.

[15] P. Liu, F. Liu, Y. Peng, Q. Wang, R. Juan, A DFT study of hydrogen adsorption on Ca decorated hexagonal B36 with van der Waals corrections, Physica E: Low-dimensional Systems and Nanostructures 114 (2019) 113576.

[16] H.M. Castro-Cruz, N.A. Macías-Ruvalcaba, Porphyrin-catalyzed electrochemical hydrogen evolution reaction. Metal-centered and ligand-centered mechanisms, Coordination Chemistry Reviews 458 (2022) 214430.

[17] C.F.N. Marchiori, G.B. Damas, C.M. Araujo, Tuning the photocatalytic properties of porphyrins for hydrogen evolution

reaction: An in-silico design strategy, Journal of Power Sources Advances 15 (2022) 100090.

[18] Z. Xia, R. Yu, H. Yang, B. Luo, Y. Huang, D. Li, J. Shi, D. Xu, Novel 2D Zn-porphyrin metal organic frameworks revived CdS for photocatalysis of hydrogen production, International Journal of Hydrogen Energy 47 (2022) 13340-50.

[19] R. Suresh, S. Vijayakumar, Adsorption of greenhouse gases on the surface of covalent organic framework of porphyrin – An ab initio study, Physica E: Low-dimensional Systems and Nanostructures 126 (2021).

[20] Q. Sun, P. Jena, Q. Wang, M. Marquez, First-Principles Study of Hydrogen Storage on Li12C60, Journal of American Chemical Society 128 (2006) 9741-5.

[21] K. Gopalsamy, V. Subramanian, Role of Alkaline Earth Metal Cations in Improving the Hydrogen-Storage Capacity of Polyhydroxy Adamantane: A DFT Study, Journal of Physical Chemistry C 120 (2016) 19932-41.

[22] M. Yoon, S. Yang, C. Hicke, E. Wang, D. Geohegan, Z. Zhang, Calcium as the Superior Coating Metal in Functionalization of Carbon Fullerenes for High-Capacity Hydrogen Storage, Physical Review Letters 100 (2008) 206806.

[23] K.I.M. Rojas, A.R.C. Villagracia, J.L. Moreno, M. David, N.B. Arboleda, Ca and K decorated germanene as hydrogen storage: An ab initio study, International Journal of Hydrogen Energy 43 (2018) 4393-400.

[24] M. Samolia, T.J.D. Kumar, Hydrogen Sorption Efficiency of Titanium-Functionalized Mg–BN Framework, Journal of Physical Chemistry C 118 (2014) 10859-66.

[25] R.Y. Sathe, S. Kumar, T.J.D. Kumar, First-principles study of hydrogen storage in metal functionalized [4,4]paracyclophane, International Journal of Hydrogen Energy 43 (2018) 5680-9.

[26] K. Gopalsamy, V. Subramanian, Hydrogen storage capacity of alkali and alkaline earth metal ions doped carbon based materials: A

DFT study, International Journal of Hydrogen Energy 39 (2014) 2549-59.

[27] G. Zhu, Q. Sun, Y. Kawazoe, P. Jena, Porphyrin-based porous sheet: Optoelectronic properties and hydrogen storage, International Journal of Hydrogen Energy 40 (2015) 3689-96.

[28] K. Srinivasu, S.K. Ghosh, Transition Metal Decorated Porphyrin-like Porous Fullerene: Promising Materials for Molecular Hydrogen Adsorption, Journal of Physical Chemistry C 116 (2012) 25184-9.

[29] S. Ghosh, J.K. Singh, Hydrogen adsorption in pyridine bridged porphyrin-covalent organic framework, International Journal of Hydrogen Energy 44 (2019) 1782-96.

[30] W. Kohn, L.J. Sham, Self-Consistent Equations Including Exchange and Correlation Effects, Physical Review 140 (1965) A1133-A8.

[31] M.J. Frisch, G.W. Trucks, H.B. Schlegel, G.E. Scuseria, M.A. Robb, J.R. Cheeseman, G. Scalmani, V. Barone, G.A. Petersson, H. Nakatsuji, X. Li, M. Caricato, A. Marenich, J. Bloino, B.G. Janesko, R. Gomperts, B. Mennucci, H.P. Hratchian, J.V. Ort, D.J. Fox, Gaussian09, Revision D.01 (2009).

[32] J-D Chai, M. Head-Gordon, Systematic optimization of long-range corrected hybrid density functionals, Journal Chemical Physics 128 2008 084106.

[33] B. Mounssef Jr, S.F.A. Morais, A.P.L. Batista, L.W. Lima, A.A.C. Braga, DFT study of H2 adsorption at Cu−SSZ−13 zeolite: a cluster approach, Physical Chemistry Chemical Physics 23 (2021) 9980-9990.

[34] N. Kobko, J.J. Dannenberg, Effect of basis set superposition error (BSSE) upon ab initio calculations of organic transition states, Journal of Physical Chemistry A 105 (2001) 1944-1950.

[35] E. Vessally, I. Alkorta, S. Ahmadi, R. Mohammadi, A. Hosseinian, A DFT study on nanocones, nanotubes (4,0), nanosheets and fullerene C60 as anodes in Mg-ion batteries, RSC Advances 9 (2019) 853-862.

[36] J. Bhuyan, K. Borah, Magnesium porphyrins with relevance to chlorophylls, Dalton Transactions 46 (2017) 6497-6509.

[37] N. Amiri, M. Hajji, T. Roisnel, G. Simonneaux, H. Nasri, Synthesis, molecular structure, photophysical properties and spectroscopic characterization of new 1D-magnesium(II) porphyrin-based coordination polymer, Research on Chemical Intermediates 44 (2018) 5583-5595.

[38] R.H. Perry, D.W. Green, In: Perry's chemical engineers handbook, seventh ed., McGraw-Hill International Editors, Sidney (1997).

[39] M.F. Fellah, Pt doped (8,0) single wall carbon nanotube as hydrogen sensor: A density functional theory study, International Journal of Hydrogen Energy 44 (2019) 27010-21.

[40] A. Ahmadi, N.L. Hadipour, M. Kamfiroozi, Z. Bagheri, Theoretical study of aluminum nitride nanotubes for chemical sensing of formaldehyde, Sensors and Actuators B Chemical 161 (2012) 1025-9.

[41] N.L. Hadipour, A.A. Peyghan, H. Soleymanabadi, Theoretical Study on the Al-Doped ZnO Nanoclusters for CO Chemical Sensors, Journal of Physical Chemistry C 119 (2015) 6398-404.

[42] A.A Peyghan, N.L. Hadipour, Z. Bagheri, Effects of Al Doping and Double-Antisite Defect on the Adsorption of HCN on a BC2N Nanotube: Density Functional Theory Studies, Journal of Physical Chemistry C 117 (2013) 2427-32.

[43] M. Eslami, V. Vahabi, A.A. Peyghan, Sensing properties of BN nanotube toward carcinogenic 4-chloroaniline: A computational study, Physica E: Low-dimensional Systems and Nanostructures 76 (2016) 6-11.

[44] P. Sjoberg, P. Politzer, Use of the electrostatic potential at the molecular surface to interpret and predict nucleophilic processes, Journal of Physical Chemistry 94 (1990) 3959-61.

[45] G. Yu, L. Lyu, F. Zhang, D. Yan, W. Cao, C. Hu, Theoretical and experimental evidence for rGO-4-PP Nc as a metal-free Fenton-like catalyst by tuning the electron distribution, RSC Advances 8 (2018) 3312-20.

[46] E. Johnson, S. Keinan, P. Mori-Sánchez, J. Contreras-García, A.J. Cohen, W. Yang, Revealing Noncovalent Interactions, Journal of American Chemical Sociesty 132 (2010) 6498-6506.